Thermal photons and dileptons

Charles Gale[a]

[a]Department of Physics, McGill University
3600 University Street, Montreal, QC, Canada H3A 2T8

We discuss the status of a subset of penetrating probes in relativistic nuclear collisions. Thermal photons and dileptons are considered, as well as the electromagnetic signature of jets.

1. Introduction

The study of penetrating probes constitutes a key aspect of the relativistic heavy ion program. In the hadronic sector, jet quenching, for example, has been a striking revelation, and has contributed to expose the qualitatively different physics that appeared in the transition from the SPS to RHIC. In this context, electromagnetic radiation also defines a privileged class of observables owing mainly to the absence of final state interactions. We briefly review some recent developments in the measurement of low- and intermediate-mass lepton pairs, and then address real photon measurements at RHIC, together with the observed supression in the hard parton spectrum.

2. Lepton pairs

2.1. Low invariant masses

At SPS energies, the measurement of low-mass lepton pairs had previously been made by the Helios/3 [1] and by the CERES [2] experimental collaborations. As a reminder of the potential of such measurements for the discovery of new physics, it is useful to write the emission rate of lepton pairs from a finite-temperature interacting system. It is [5]

$$E_+E_-\frac{d^6R_{\ell^+\ell^-}}{d^3p_+d^3p_-}=\frac{2e^2}{(2\pi)^6}\frac{n_{\rm B}(E,T)}{M^4}L^{\mu\nu}{\rm Im}\Pi^{\rm R}_{\mu\nu} \tag{1}$$

where $n_{\rm B}$ is a Bose-Einstein distribution function, $L^{\mu\nu}$ is a lepton tensor, and ${\rm Im}\Pi^{\rm R}_{\mu\nu}$ is the imaginary part of the in-medium, retarded, finite-temperature self-energy of the photon. Furthermore, in the nonperturbative sector, Vector Meson Dominance (VMD) relates the photon self-energy to the in-medium vector spectral density. It is therefore clear that the measurement of the low-mass spectrum of lepton pairs can reveal pristine features of the interacting many-body system. In this regard, the situation before this conference was summarized in a presentation of the CERES collaboration [2], where three theoretical approaches were shown to be consistent with the data. Those were (i) a many-body calculation where the in-medium spectral densities are altered owing to their coupling with a variety of states accessed through interactions with a hot and dense hadronic ensemble [6]; (ii) An effective chiral model, where strong precursor effects already manifest themselves in a shifting of hadronic masses at intermediate baryonic densities [7]; (iii) A simple thermal parametrization of the quark-antiquark annihilation Born rates, justified by a duality argument [8]. Finally and importantly, approaches solely based on vacuum properties have difficulty providing an interpretation of the CERES measurements.

It is probably fair to write that one of the highlights of the Quark Matter 2005 meeting has been the disclosure of the new NA60 data [3] for In-In collisions at the CERN SPS. The low-mass dilepton component of this experiment's measurements is of exceptional quality and statistics [3,4]. The experimental collaboration also has shown a comparison with their data with the results of approaches (i) and (ii), above. On the basis of that comparison, the experimental data strongly suggest that large mass shifts of the vector mesons are not observed. This same comparison also shows consistency with the many-body calculations of (i) above. An immediate conclusion is the following: NA60 data are now precise enough to distinguish between different approaches, or at least between some of the more extreme scenarios. This is important progress, and represents a great stride forward. Whether this rules out or not entire classes of models will remain to be seen, but one point is clear: the approach shown by the experimental collaboration which is based on in-medium mass shifts *is the same one that was in agreement with CERES results* [6]. It is entirely possible that theoretical refinements are needed in order to be in line with evolving theoretical paradigms, but the fact remains that any single theory now has to deal with two separate experimental results.

The low-mass results do signal an unambiguous many-body effect. To go beyond this to a state of deeper theoretical understanding is not an easy talk. For example, one of the original aims of this whole experimental program was to isolate a signal (precursor or not) of chiral symmetry restoration. This goal has unfortunately remained elusive, owing largely to the difficulty of directly extracting an axialvector correlator from relativistic heavy ion data. In the chiral limit, vector and axialvector correlators are constrained by sum rules of the Weinberg-type [9], and these may be realized in several different ways [10]. The ability to chart a path to correlator degeneracy (in the Weinberg sense) would definitely represent a significant breakthrough. However, the precise data shown at this meeting will surely fuel many investigations.

2.2. Intermediate invariant masses

The study of lepton pair production at intermediate masses ($m_\phi < M < m_{J/\psi}$) are especially interesting in the context of searches for the quark-gluon plasma, as kinematical arguments combined with the original high temperature of the QCD plasma would designate the intermediate invariant mass region as a window of opportunity for the observation of plasma radiation [11,12]. In this context, considerable interest was generated by the fact that an excess over sources expected from pA measurements has been confirmed in the intermediate mass region by the Helios/3 [1] and NA50 [16] collaborations. This excess could in turn signal an increase in $c\bar{c}$ abundances, which would then manifest itself through the correlated semileptonic decays of open charm mesons. Alternatively, thermal lepton pairs need to be ruled out as viable scenario before other explanations be invoked. Those thermal sources are akin to the ones identified in the low dilepton mass

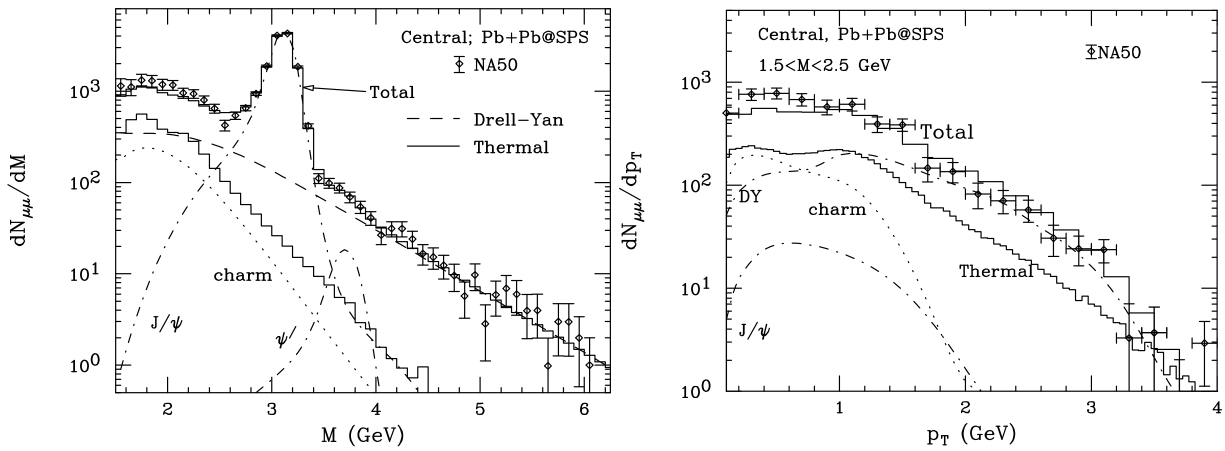

Figure 1. The invariant mass and momentum spectra, calculated for dimuon pairs. The sources are Drell-Yan, correlated charm decay, and thermal (quark-gluon plasma and hadron gas). The full curve histogram is the sum of all of those different contributions, after correcting for detector acceptance, resolution, and efficiency.

sector by the many-body calculations. Showing that they also shine at higher invariant masses would go a long way in providing a consistent picture of electromagnetic radiation in heavy ion collisions. In the theoretical interpretation of such data, a potential caveat is lurking, and is related to the use of effective Lagrangian techniques. These rely on physical parameters which were essentially all fitted in regions characterized by soft energy scales, and had mostly to do with strong and electromagnetic decay widths. When moving over to larger invariant masses, off-shell effects will set in, making controlled extrapolations a problem [13]. Fortunately, there exists a wealth of data of the type $e^+e^- \rightarrow$ hadrons, which cover precisely the same range in invariant mass as the heavy ion data [14]. These data can be analyzed channel-by-channel and have been used, together with τ-decay measurements, to construct the vector and axial vector spectral densities that can be related to the lepton pair spectrum [15]. Summing all kinematically-relevant channels, one arrives at a source which may be compared to the data via the space-time modeling of the nuclear collision. The result of one such exercise is shown in Figure 1. It is fair to write that the specific values of the temperature evolution, for example, depend somewhat on the particularities of the space-time modeling. However, a fairly robust conclusion still emerges: the intermediate-mass NA50 data does not demand a large contribution from plasma radiation (it is about 20% here), nor does it need a large enhancement of the initial charm content. Even though specific details do differ, this conclusion is shared by other theoretical studies of a similar nature [17–19]. However, in order to bring this situation to some degree of closure, a direct measurement of the strangeness component would go a long way. This has now been done and has been reported at this conference by the NA60 collaboration [3,20]. The first measures taken by the collaboration was to experimentally confirm the presence of an enhancement in the intermediate-mass continuum in nuclear collisions, over what is seen in proton-nucleus events. However, with the new information provided by the muon offset measurement, NA60 can now assert that the excess is not linked with open charm enhancement. This new data is also compatible with the excess that had previously been observed by NA50. The analysis will proceed further, but it already reveals that the signal that exceeds what is associated with pA sources increases faster than linearly with the number of participants. The statistics will improve, the 2004 proton-nucleus data will be analyzed and such measurements are important for the determination of QCD effects beyond leading-twist [22]. It is however clear that these results do represent a great leap in our quest for a complete quantitative understanding of the electromagnetic radiation being produced in relativistic nuclear collisions.

3. Photons from jet-plasma interactions

One of the most striking findings of the RHIC program is the strong apparent modification of jet characteristics, following a passage through an interacting, dense medium [21]. A compelling theoretical interpretation of these results is that of jet absorption, signaling in effect the existence of a hot and dense partonic phase. Several models of jet-quenching through gluon bremsstrahlung have been elaborated [23–27]. Here, we use that of AMY [28], because of its potential to handle consistently jet energy loss and photon emission. In this approach, Fokker-Planck equations are solved to obtain the time-evolution of the initial hard gluon, $P_g(p, t = 0)$ and hard quark plus antiquark distributions, $P_{q\bar{q}}(p, t = 0)$. The coupled equations are

$$\begin{aligned}
\frac{dP_{q\bar{q}}(p)}{dt} &= \int_k P_{q\bar{q}}(p+k)\frac{d\Gamma^q_{qg}(p+k,k)}{dkdt} - P_{q\bar{q}}(p)\frac{d\Gamma^q_{qg}(p,k)}{dkdt} + 2P_g(p+k)\frac{d\Gamma^g_{q\bar{q}}(p+k,k)}{dkdt} \\
\frac{dP_g(p)}{dt} &= \int_k P_{q\bar{q}}(p+k)\frac{d\Gamma^q_{qg}(p+k,p)}{dkdt} + P_g(p+k)\frac{d\Gamma^g_{gg}(p+k,k)}{dkdt} \\
&\quad - P_g(p)\left(\frac{d\Gamma^g_{q\bar{q}}(p,k)}{dkdt} + \frac{d\Gamma^g_{gg}(p,k)}{dkdt}\Theta(2k-p)\right) \qquad (2)
\end{aligned}$$

The kernels $d\Gamma(p,k)/dkdt$ are the transition rates, and they contain the resummation effects typical of interactions with a thermal medium [28]. The solution of the joint equations for the time-evolution of the parton distribution functions permits the modeling in real time of the partonic spectra. The hard parton can then fragment into the different varieties of observed particles. Up to suppressed corrections, the cross section for produced pions in nucleon-nucleon collisions can be written in a factorized form as

$$\frac{d^3\sigma_{\rm pp}}{d^2p_\perp dy} = \sum_{a,b,c,d}\int dx_a dx_b\, g(x_a,Q)g(x_b,Q)K_{\rm jet}\frac{d\sigma^{a+b\to c+d}}{dt}\frac{1}{\pi z}D_{\pi^0/c}(z,Q')\ , \qquad (3)$$

where $g(x,Q)$ is the parton distribution function in a nucleon, $D_{\pi^0/c}$ is the pion fragmentation function, $d\sigma^{ab\to cd}/dt$ is the parton-parton cross section at leading order, and $K_{\rm jet}$ accounts for higher order effects. Here, "jet" essentially means a fast parton with $p_T \gg$ 1 GeV. This procedure, with the factorization scale (Q) and the fragmentation scale (Q') set equal to p_T, the CTEQ5 parton distribution functions, and $K_{\rm jet} \sim 1.7$, does a very good job of reproducing the measured π^0 above $p_T \approx 5$ GeV [29], in nucleon-nucleon collisions at RHIC. This is shown in Figure 2.

To obtain the high p_T π^0 cross section in AA collisions, the pp calculation must be modified in two important ways. First, the parton distribution function of a nucleus differs from that of a proton:

$$g_{\rm A}(x_a,Q) = g(x_a,Q)R_{\rm A}(x_a,Q) \qquad (4)$$

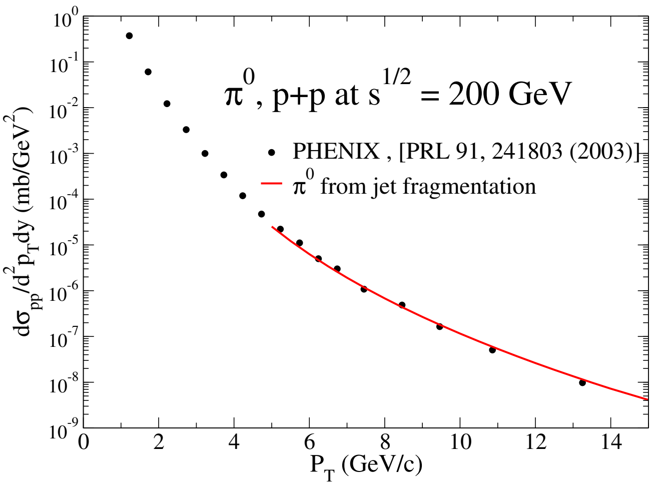

Figure 2. Neutral pion spectra in pp collisions at RHIC. The data points are from PHENIX, and the calculated results are from jet fragmentation.

The nuclear modification factor of the structure function $R_{\rm A}$ takes into account shadowing and anti-shadowing [30]. Also, the hard parton looses energy between the initial hard scattering and its hadronization, and this information in contained in the time-evolution of the entire partonic profile we have described earlier. The π^0 spectrum obtained in AA collisions is then

$$\frac{d^3N_{\rm AA}}{dyd^2p_T} = \frac{\langle N_{\rm coll}\rangle}{\sigma_{\rm in}} \sum_{a,b,c,d} \int dx_a dx_b g_{\rm A}(x_a,Q) g_{\rm A}(x_b,Q) K_{\rm jet} \frac{d\sigma^{a+b\to c+d}}{dt} \frac{\tilde{D}_{\pi^0/a}(z,Q)}{\pi z} \tag{5}$$

where $\langle N_{\rm coll}\rangle$ is the average number of binary collisions, $\sigma_{\rm in}$ is the inelastic nucleon-nucleon cross section, and the medium-modified fragmentation function is

$$\tilde{D}_{\pi^0/c}(z,Q) = \int d^2r_\perp \mathcal{P}(\mathbf{r}_\perp) \tilde{D}_{\pi^0/c}(z,Q,\mathbf{r}_\perp,\mathbf{n}) \tag{6}$$

where $\mathcal{P}$ takes into account the geometry of the emitting source, and

$$\tilde{D}_{\pi^0/c}(z,Q,\mathbf{r},\mathbf{n}) = \int dp_f \, \frac{z'}{z} \left(P_{q\bar{q}/c}(p_f;p_i) D_{\pi^0/q}(z',Q) + P_{g/c}(p_f;p_i) D_{\pi^0/g}(z',Q) \right) \tag{7}$$

where $z = p_T/p_i$, and $z' = p_T/p_f$. Note also that $P_{q\bar{q}/c}(p_f;p_i)$ and $P_{g/c}(p_f;p_i)$ are the solutions to the Fokker-Planck equation and represent the probability to get a given parton with final momentum p_f, given that the initial configuration is a particle of type c and momentum p_i. Information on the initial temperature sensitivity, on the geometry and other details is in Ref. [29].

A quantitative measure of in-medium modifications is contained in the so-called R_{AA} profile

$$R_{AA} = \frac{\sigma_{\rm in} d^3N_{AA}/dyd^2p_T}{\langle N_{coll}\rangle d^3\sigma_{pp}/dyd^2p_T} \ , \tag{8}$$

when plotted as a function of the transverse momentum. Clearly, if a nucleus-nucleus collision is nothing but a superposition of nucleon-nucleon collisions, then R_{AA} should be

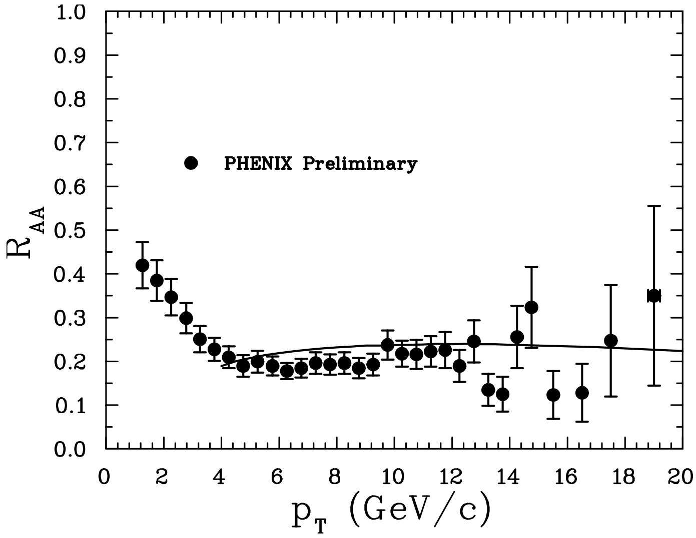

Figure 3. The ratio R_{AA} for π^0, as a function of transverse momentum. The full line is the calculation described in this text, and in [29], with $\alpha_s = 0.34$. The initial temperature is 370 MeV, and is consistent with the study in [31]. Data are from [32].

unity. This variable is now available for a variety of particles, over a wide range of transverse momenta. Figure 3 reveals new preliminary data, where the behavior of R_{AA} over an impressive range of almost 20 GeV/c is shown. Also there, is the result of a calculation with the formalism described here. In this approach, the strong coupling constant, α_s, is a free parameter. In his plot, a value of $\alpha_s = 0.34$ yields a good fit. This value is kept fixed for the rest of this work. Further note there are uncertainties associated with the determination of $< N_{\rm coll} >$, as well as inherent systematic measurement uncertainties. This combination roughly is of the order of 10%. The apparent agreement (for $p_T \geq 4$ GeV) is at least superficially satisfying, even if many questions remain on details of the opacity of the medium, and on the actual sensitivity of this variable on bulk properties. The answer to those questions is at present scheme-dependent. With data of this quality however, the next meeting in this series is bound to see progress on these issues. Nevertheless, the flatness of these spectra appears a robust feature. The softer part of the spectrum is not reproduced by a QCD fragmentation framework and requires additional ingredients possibly related to parton recombination [33].

With the machinery at hand, the spectrum of photons produced in nucleus-nucleus collisions can be calculated, including those originating for jet-plasma interactions [34], but consistently taking account energy-loss systematics. The sources include those active in pp collisions: the direct photons produced by parton Compton and annihilation events, and the fragmentation photons produced by bremsstrahlung from final state partons. In AA collisions, the sources above still operate but the fragmenting jets are now subject to energy-loss considerations. In addition, hard partons traveling in the medium can also produce photons through medium-induced bremsstrahlung. Finally, the conversion of leading partons to photons [34,29] was found to be a significant contribution and should be treated consistently with the other channels enumerated here. The different sources for Au + Au collisions at RHIC are shown in Figure 4. The agreement with the recent PHENIX photon data is very good. Furthermore, it is satisfying to note that the modeling

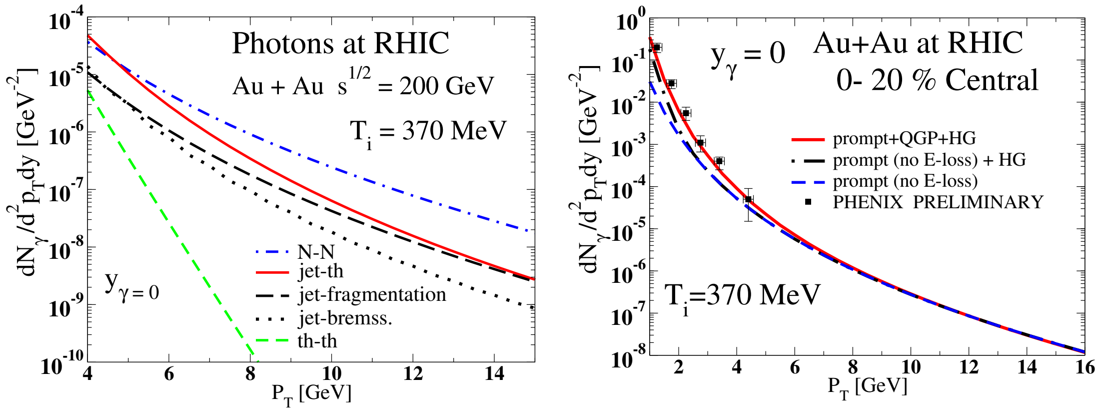

Figure 4. Left Panel: Contributing sources of high-p_T photons at mid-rapidity in central nuclear collisions at RHIC. Solid line: jet-photon conversion in the plasma; dotted line: bremsstrahlung from jets in the plasma; short dashed line: thermal photons [31]; long dashed line: photons from fragmenting jets; dot-dashed line: contribution from the primordial hard scattering. Right panel: Total production of photons at RHIC, compared with new PHENIX data [35]. The solid line represents all processes from the left panel together with photons from the hadronic gas (HG) [31]; the dot-dashed line do not include any plasma-related contributions but has those from the HG. Photons from pp collisions scaled to AA are shown by the dashed lines.

parameters were fixed prior to its release [29]. Further note that when the jet-photon conversions are omitted, the total photon production is reduced by up to 45% around $p_T = 3$ GeV/c, showing the importance of this process. The total plasma contribution appears important for $p_T < 6$ GeV/c. Here also, the quality of this data opens the door to additional investigations. Some have been done [36] and more will follow, but importantly, electromagnetic signals and hard hadronic probes are no longer disjoint observables.

4. Conclusion

It is not an overstatement to write that the measurement of electromagnetic probes in relativistic has produced some very exciting results. All expectations are that this will continue, with larger statistics samples and the measurement of lepton pairs at RHIC. With the data shown at this meeting, we are entering an era of precision measurements and modeling. For example, measurements of photon azimuthal asymmetry are now at reach.

Acknowledgments

I am grateful to all of my collaborators for their involvement with any aspect of the work presented here. Of those, I also thank Simon Turbide for a critical reading of this manuscript. This work was supported in part by the Natural Sciences and Engineering Research Council of Canada, and in part by the Fonds Nature et Technologies of the Government of Quebec.

REFERENCES

1. M. A. Mazoni *et al.*, Nucl. Phys. **A566** (1994) 95c; M. Masera *et al.*, Nucl. Phys. **A590** (1995) 93c; A. L. S. Angelis *et al.*, Eur. Phys. J. C **13** (2000) 433.
2. D. Miśkowiec, these proceedings.
3. E. Scomparin, these proceedings
4. S. Damjanovic, these proceedings.
5. H. A. Weldon, Phys. Rev. D **42** (1990) 2384; Charles Gale and Joseph I. Kapusta, Nucl. Phys. **B357** (1991) 65.
6. R. Rapp and J. Wambach, Adv. Nucl. Phys. **25** (2000) 1.
7. See, for example, G. E. brown and Mannque Rho, Phys. Rep. **363** (2002) 85.
8. K. Gallmeister *et al.*, Nucl. Phys. **A715** (2003) 705.
9. S. Weinberg, Phys. Rev. Lett. **18** (1987) 507.
10. J. I. Kapusta and E. V. Shuryak, Phys. Rev. D **49** 46944704 (1994).
11. E. V. Shuryak, Phys. Lett. B **78** (1978) 150.
12. K. Kajantie, J. Kapusta, L. McLerran, and A. Mekjian, Phys. Rev. D **34** (1986) 2746.
13. S. Gao and C. Gale, Phys. Rev. C **57** (1998) 254.
14. See, for example, S. I. Dolinsky *et al.*, Phys. Rep. **202** (1991) 99, and references therein.
15. Z. Huang, Phys. Lett. B **361** (1995) 131, and private communication.
16. M. C. Abreu *et al.*, Eur. Phys. J. C **14** (2000) 443.
17. G. Q. Li and C. Gale, Phys. Rev. Lett. **81** (1998) 1572; Phys. Rev. C **58** (1998) 2914.
18. R. Rapp and E. V. Shuryak, Phys. Lett. B **473** (2000) 13.
19. K. Gallmeister, B. Kämpfer, and O. P. Pavlenko, Phys. Lett. B **473** (2000) 20.
20. R. Shahoyan, these proceedings.
21. X.-N. Wang, these proceedings.
22. See, for example, Jan-Wei Qiu, Eur. Phys. J. C **43** (2005) 239.
23. R. Baier, Y. L. Dokshitzer, A. H. Mueller, S. Peigné, and D. Schiff, Nucl. Phys. **B484** (1997) 291; R. Baier, Y. L. Dokshitzer, A. H. Mueller, and D. Schiff, JHEP **0109** (2001) 33.
24. E. Wang and X.-N. Wang, Phys. Rev. Lett. **89** (2002) 162301.
25. I. Vitev and M. Gyulassy, Phys. Rev. Lett. **89** (2002) 252301.
26. A. Kovner and U. A. Wiedemann, *QGP3*, R. Hwa and X.-N. Wang, editors (World Scientific, Singapore, 2003).
27. B. G. Zakharov, JETP lett. **63** (1996) 952; *ibid.* **65** (1997) 615; *ibid.* **70** (1999) 176.
28. P. Arnold, G. D. Moore, and L. G. Yaffe, JHEP **0111** (2001) 57; JHEP **0206** (2002) 30.
29. S. Turbide, C. Gale, S. Jeon, and G. D. Moore, Phys. Rev. C **72**, 014906 (2005).
30. K. J. Eskola, V. J. Kolhinen, and C. A. Salgado, Eur. Phys. J C **9**, 61 (1999).
31. S. Turbide, R. Rapp, and C. Gale, Phys. Rev. C **69**, 014903 (2004).
32. B. Cole, these proceedings.
33. D. Molnár, these proceedings.
34. R. J. Fries, B. Müller, and D. K. Srivastava, Phys. Rev. Lett. **90**, 132301 (2003).
35. H. Buesching, these proceedings.
36. D. d'Enterria and D. Peressounko, nucl-th/0503003.